Catal Lett (2012) 142:1167–1174
DOI 10.1007/s10562-012-0889-y

ORIGINAL ARTICLE

N_2O Mitigation in a Coupled LNT–SCR System

Jin Wang · Mark Crocker

Received: 18 May 2012 / Accepted: 2 August 2012 / Published online: 17 August 2012

Abstract N_2O formation and consumption were investigated over a coupled LNT–SCR system consisting of a low-precious metal loaded Pt/Rh LNT catalyst and a commercial Cu–zeolite SCR catalyst. Under lean–rich cycling conditions, N_2O emissions from the LNT were found to be partially mitigated by the downstream SCR catalyst. N_2O decomposition over the SCR catalyst was observed in the absence of reductant immediately after the switch to rich conditions, while N_2O reduction occurred after subsequent breakthrough of the reductant from the LNT. Steady-state data indicate that the former process is weakly promoted by NO which breaks through the LNT at the same time as the N_2O. Steady-state experiments revealed the order $H_2 > NH_3 > CO > C_3H_6$ for the efficacy of N_2O reduction with different reductants. These findings suggest that coupled LNT–SCR systems can not only improve overall NO_x conversion levels but can also mitigate N_2O emissions from the LNT catalyst under actual driving conditions.

Keywords LNT–SCR · Nitrous oxide · N_2O, SCR catalyst · Cu–zeolite · Reductant

1 Introduction

The use of lean-burn engines in vehicle applications is increasing due to their higher fuel efficiency and lower CO_2 emissions compared with stoichiometric engines. However, the efficient abatement of NO_x in lean-burn conditions represents a significant challenge that must be tackled in order to meet increasingly stringent emission regulations. Lean NO_x traps (LNTs) and selective catalytic reduction (SCR) have been developed to help meet these regulations. LNT catalysts, which store NO_x during lean operation and then facilitate reduction of the stored NO_x under subsequent rich conditions, have been successfully developed for lean-burn engines, especially for light duty diesel and gasoline lean-burn applications [1]. SCR, which employs a catalyst to facilitate NO_x reduction by urea-derived NH_3 in the presence of excess of O_2, has been commercialized for light and heavy duty diesel engines [2].

Recently, a number of studies have been published which demonstrate that the performance of LNT catalysts can be significantly improved by adding a SCR catalyst in series downstream [3–12]. In the combined LNT–SCR system, NH_3 is generated in the upstream LNT during rich purges and subsequently stored on the SCR catalyst where it reacts with NO_x that breaks through the LNT during lean operation. Compared with LNT- or SCR-only systems, the LNT–SCR approach has several advantages. The downstream SCR catalyst not only improves overall NO_x conversion, but also eliminates NH_3 slip from the LNT catalyst. Moreover, since the presence of the SCR catalyst relaxes the NO_x conversion requirements of the LNT catalyst, the volume of the LNT in the LNT–SCR system can, in principle, be lower than for an LNT-only system, thereby reducing the precious metal costs. Furthermore, the need for a urea injection system is eliminated.

In a recent report we showed that in addition to the NH_3 pathway for NO_x conversion, a second pathway can operate in the SCR catalyst of LNT–SCR systems which is associated with the presence of hydrocarbons in the rich phase [12]. According to adsorption experiments, significant co-adsorption of NH_3 and propene occurred in the SCR

J. Wang · M. Crocker (✉)
Center for Applied Energy Research, University of Kentucky, Lexington, KY 40511, USA
e-mail: mark.crocker@uky.edu

catalyst, while under lean–rich cycling conditions the contributions of NH_3 and C_3H_6 to NO_x conversion were found to be essentially additive. These findings suggest that under actual driving conditions, NO_x reduction by hydrocarbons in the SCR catalyst can contribute to the mitigation of lean and rich phase NO_x. In these experiments, we also observed a hitherto unreported benefit for LNT–SCR systems, namely the partial elimination of N_2O slip from the LNT by the SCR catalyst. It is common knowledge that N_2O plays an important role in the destruction of the ozone layer in the stratosphere [13, 14]. Furthermore, the N_2O molecule is quite stable in the atmosphere and the greenhouse potential of N_2O is about 300 times higher than that of CO_2 [15]. Consequently, from an environmental standpoint, the control of N_2O emissions is of increasing importance.

A number of published studies [16–21] have addressed the issue of N_2O formation in LNT catalysts during lean–rich cycling experiments. The catalytic decomposition of N_2O over metal ion-exchanged zeolite catalysts has also been reported, as well its SCR by NH_3, CO, H_2 or hydrocarbons over these same catalysts [22–34]. However, to the best of our knowledge, studies concerning N_2O formation and reduction in coupled LNT–SCR systems have not been reported. In this paper we present data concerning N_2O formation over the LNT part of the system, and its decomposition over the downstream SCR catalyst.

2 Experimental

2.1 Catalysts

Two catalysts were used in this study, comprising a low-precious metal loaded Pt/Rh LNT catalyst and a commercial SCR catalyst of the Cu–chabazite type. The LNT catalyst contained BaO as the main NO_x storage material, as well as a ceria-based oxygen storage material, and Pt and Rh as the precious metals. Both catalysts were provided by BASF and were prepared on 400 cpsi/6.5 mil ceramic monoliths. For bench reactor tests, 7.5 cm (l) × 2.1 cm (d) core samples of each catalyst were drilled from the monoliths.

2.2 LNT–SCR Lean–Rich Cycling Experiments

Catalyst tests were performed on a synthetic gas bench reactor. The LNT and SCR monolith cores were wrapped in Zetex insulation tape and placed in separate vertical reactor tubes (2.2 cm inner diameter) which were independently heated by two electric furnaces. Details concerning the reactor configuration and product analysis system can be found in a previous paper [12]. Briefly, the catalysts were positioned in series, the inlet face of the SCR catalyst monolith being 10″ downstream of the outlet face of the LNT monolith. A gas sampling port was positioned between the catalysts to enable analysis of the effluent gas from the LNT catalyst. A rapid switching 4-way valve system was used to alternate between the lean and rich gas mixtures so that the lean/rich/lean transitions in these experiments were almost instantaneous (within 0.2 s). K-type thermocouples were placed at the LNT inlet, mid-point and exit, and the SCR catalyst inlet and outlet, to monitor the temperature profiles. A multi-gas analyzer (MKS Model 2030) was used to monitor the concentrations of NO, NO_2, N_2O, NH_3, C_3H_6, CO, CO_2, and H_2O between the LNT and SCR catalysts, as well as at the inlet of the LNT and at the outlet of the SCR catalyst. During lean–rich cycling, the observed catalyst breakthrough profiles stabilized to a fixed limit cycle in about 2 h, at which point it was possible to characterize the performance in terms of the 'stationary' concentration cycles. Data were collected in the range 150–450 °C using the gas compositions summarized in Table 1. Note that relatively low reductant concentrations were used in these experiments, in order to highlight differences in the NOx conversion of the LNT and LNT–SCR systems. The selectivity to N_2O was calculated according to:

$$S_{N_2O}(\%) = 100 \times \frac{2\int_0^t [N_2O]dt}{\int_0^t ([NO_x]_0 - [NO_x])dt}$$

N_2O conversion over the SCR catalyst during these experiments was calculated according to:

$$N_2O\,\text{conversion}\,(\%) = 100 \times \left([N_2O]_{\text{inlet}} - [N_2O]_{\text{outlet}}\right)/[N_2O]_{\text{inlet}},$$

where all concentrations are cycle-averaged, integrated values (in ppm s). Before beginning the measurements, catalysts were de-greened by exposing them to lean–rich cycling conditions at 500 °C for 5 h, using the lean gas feed and the rich gas mixture #3 shown in Table 1.

2.3 N_2O Reduction Experiments Over SCR Catalyst Under Continuous Flow Conditions

Experiments were performed in the synthetic gas bench reactor described above using a 7.5 cm (l) × 2.1 cm (d) monolith sample of the SCR catalyst. The total feed gas flow rate was set to 13,719 sccm, giving a GHSV of 30,000 h^{-1}. Two K-type thermocouples were placed just before the SCR catalyst and at the catalyst outlet to monitor the temperature profile. The catalyst was pre-treated in a flowing mixture of 8 % O_2, 5 % CO_2, 5 % H_2O and N_2 (balance) at 500 °C for 3 h, after which the catalyst was cooled to 150 °C under a flowing feed of 5 % CO_2, 5 %

Table 1 Base conditions used for NO_x storage-reduction cycling experiments

Parameter	Lean	Rich #1	Rich #2	Rich #3
Duration (s)	60	5	5	5
Temperature (°C)	150–450	150–450	150–450	150–450
Space velocity (h^{-1})	30,000	30,000	30,000	30,000
NO (ppm)	300	300	300	300
O_2 (%)	8	0	0	0
CO (%)	–	1	–	–
C_3H_6 (ppm)	–	–	3,333	–
H_2 (%)	–	–	–	1
CO_2 (%)	5	5	5	5
H_2O (%)	5	5	5	5
N_2 (%)	Balance	Balance	Balance	Balance

H_2O and N_2 (balance). At this point N_2O (100 ppm), H_2O (as indicated) and the reductant (1 % H_2, 1 % CO, 3,333 ppm C_3H_6, 6,666 ppm NH_3, or the indicated amount of NO) were added to the feed. N_2O conversion measurements were performed under steady-state conditions at intervals of 50 °C in the temperature range 150–500 °C.

3 Results and Discussion

3.1 NO_x Conversion and N_2O Selectivity of LNT and Coupled LNT–SCR Catalyst Systems

Lean/rich cycling experiments with different reductants were performed over a coupled LNT–SCR system using different feed gas compositions in the rich phase (see Table 1). Figure 1 shows the NO_x removal efficiency and selectivity to N_2O obtained with 1 % CO as the reactant over the single LNT and over the coupled LNT–SCR system at different LNT catalyst inlet temperatures. Note that the inlet temperature of the SCR catalyst in these experiments was typically 20–65 °C higher than that of the LNT catalyst, due to the exotherm resulting from the lean–rich cycling. Under these conditions (rich phase condition #1 in Table 1), the NO_x removal efficiency of the coupled LNT–SCR system is always higher than that of the LNT catalyst at temperatures in the range 150–450 °C, a fact which can be ascribed to the utilization of NH_3 slip from the LNT for NO_x reduction over the SCR catalyst (data not shown). Simultaneously, a decrease is observed in N_2O emissions from the LNT–SCR system as compared to the LNT-only configuration. This is reflected in the decreased overall system selectivity to N_2O, which is also depicted in Fig. 1. Indeed, N_2O emitted by the LNT is increasingly reduced by the SCR catalyst at temperatures in excess of 220 °C (this number representing the LNT inlet temperature). For example, at 184 °C, the selectivity to N_2O is 75 % over the LNT catalyst, decreasing to 66 % after the

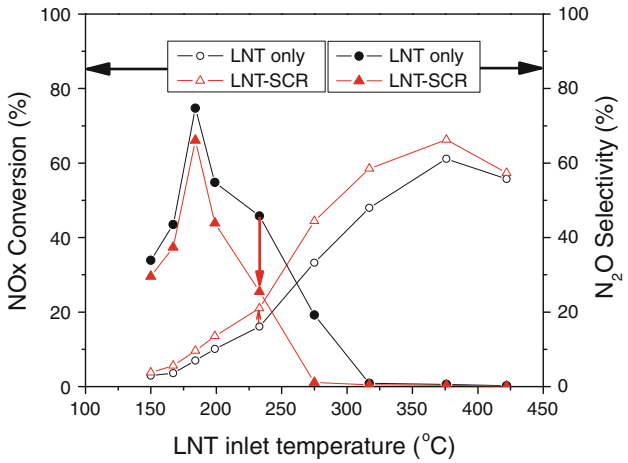

Fig. 1 Comparison of cycle-averaged NO_x conversion and selectivity to N_2O for LNT-only and LNT–SCR systems using 1 % CO as reductant

SCR catalyst, while at 233 °C the corresponding values are 46 % and 25 %.

Using C_3H_6 as the reducing agent (rich condition #2 in Table 1), the benefit of the SCR catalyst with respect to NO_x conversion is again apparent. However, comparing Fig. 2 with Fig. 1, it is apparent that significant differences exist between the two experiments with respect to N_2O selectivity. When CO is the reductant (Fig. 1), the N_2O selectivity over the LNT catalyst is very high at low temperatures. Initially it increases with increasing temperature, reaching a maximum of 75 % at 184 °C, and then decreases with further increase of the temperature. In the case that C_3H_6 is used as the reductant, the N_2O selectivity over the LNT reaches an initial maximum at 275 °C (32 %), followed by a second maximum (20 %) upon increase of the temperature to 376 °C. In these experiments, NO (500 ppm) was present in both the lean and rich phases; notably, when NO was omitted from the rich phase, evolution of N_2O was not observed at the higher

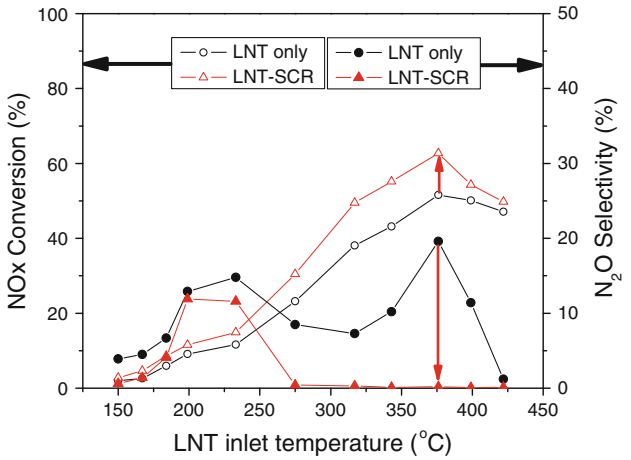

Fig. 2 Comparison of cycle-averaged NO_x conversion and selectivity to N_2O for LNT-only and LNT–SCR systems using 3,333 ppm C_3H_6 as reductant

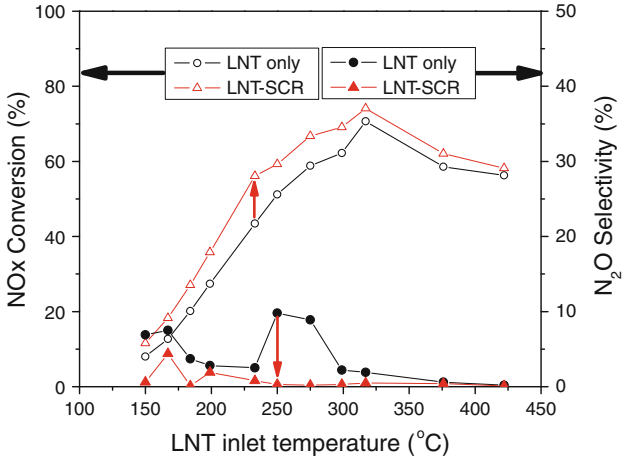

Fig. 3 Comparison of cycle-averaged NO_x conversion and selectivity to N_2O for LNT-only and LNT–SCR systems using 1 % H_2 as reductant

temperature (data not shown). From this it can be inferred that the low and high temperature N_2O selectivity maxima correspond to NO_x reduction processes involving stored NO_x and gas phase NO_x, respectively. Given that at low temperatures ceria contributes significantly to NO_x storage [35], it can be speculated that under reducing conditions the cerium nitrates are decomposed at low temperatures with appreciable formation of N_2O. Adsorption and reaction of gas phase NO appears to be a kinetically slower path to N_2O and therefore becomes significant at higher temperatures. As for the case with CO, Fig. 2 indicates that significant N_2O conversion occurs over the SCR catalyst in the LNT–SCR system.

For the case of H_2 (rich condition #3 in Table 1), the NO_x conversion and N_2O selectivity for the LNT-only and coupled LNT–SCR systems are shown in Fig. 3. As expected, H_2 is the best NO_x reductant at all temperatures, while the benefit of the SCR catalyst is again apparent with respect to system NO_x conversion and the abatement of N_2O emissions. N_2O selectivity is shown in Fig. 3 and is very low, peaking at a value of 8 % at 165 °C and then attaining a second maximum of 10 % at 250 °C. As for the case when C_3H_6 was used as reductant, the high temperature maximum disappeared when NO was removed from the rich phase feed gas, again indicating that it is associated with the reduction of gas phase NO.

3.2 N_2O Conversion Over SCR Catalyst Under Lean–Rich Cycling

It should be noted that N_2O selectivity for the LNT-only and LNT–SCR systems in the above experiments is calculated based on the N_2O slip from the LNT or SCR catalyst, divided by the corresponding amount of NO_x

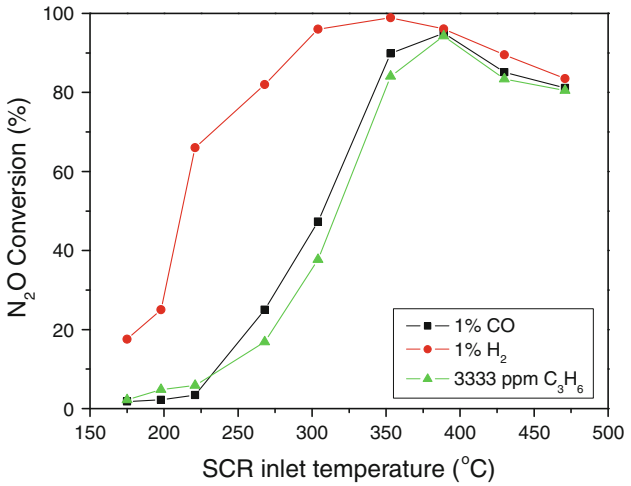

Fig. 4 Cycle-averaged N_2O conversion over SCR catalyst in LNT–SCR configuration. Feed: lean (60 s): 300 ppm NO, 8 % O_2, 5 % CO_2, 5 % H_2O, N_2 as balance; rich (5 s): 300 ppm NO, 1 % H_2 or 1 % CO or 3,333 ppm C_3H_6 as reductant, 5 % CO_2, 5 % H_2O, N_2 as balance; GHSV = 30,000 h^{-1}

converted. Since the overall NO_x conversion is improved by the SCR catalyst, a drop in calculated N_2O selectivity can result even when there is no change in the N_2O slip from the SCR catalyst. Therefore, to clarify the contribution of the SCR catalyst, the calculated N_2O conversions over the SCR catalyst are displayed as a function of temperature in Fig. 4. From these results it is evident that the nature of the reductant plays a significant role in determining the extent of N_2O destruction, H_2 being more effective as a reductant than CO or C_3H_6. Noteworthy too is the fact that CO or C_3H_6 breakthrough (from the LNT) was not observed at temperatures above 400 °C; this explains why the N_2O conversion in Fig. 4 tails off above

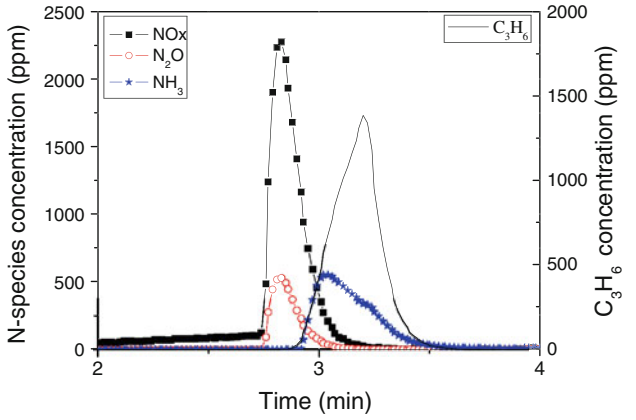

Fig. 5 NO_x, N_2O, NH_3 and C_3H_6 concentrations at LNT outlet as a function of time during rich purging (LNT inlet temperature = 375 °C). Feed: lean (360 s): 300 ppm NO, 8 % O_2, 5 % CO_2, 5 % H_2O, N_2 as balance; rich (30 s): 300 ppm NO, 3,333 ppm C_3H_6 as reductant, 5 % CO_2, 5 % H_2O, N_2 as balance; GHSV = 30,000 h^{-1}

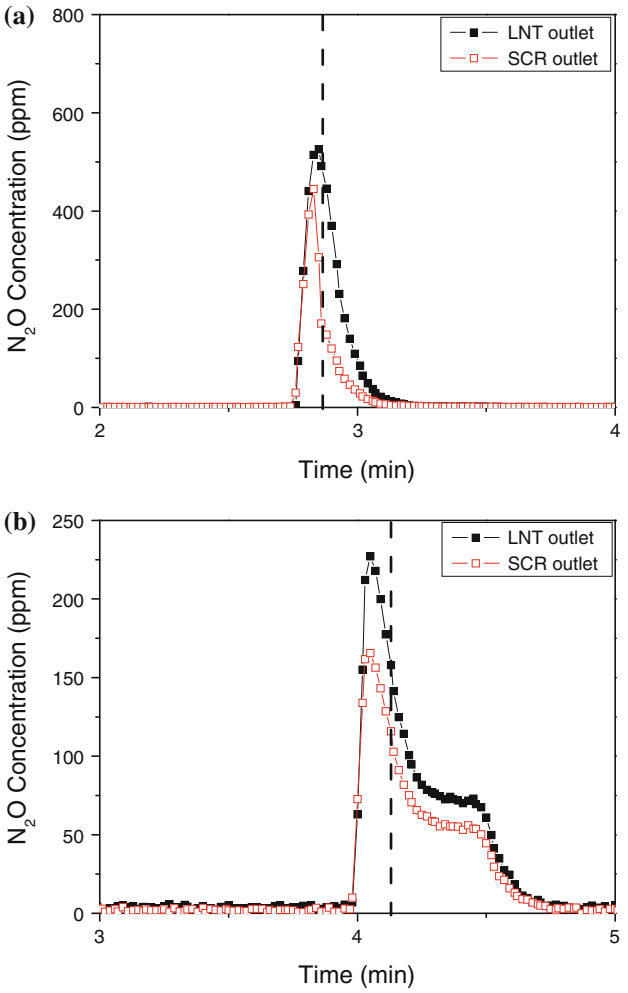

Fig. 6 Expanded view of N_2O concentration at LNT and SCR catalyst outlets as a function of time during rich purging: **a** 3,333 ppm C_3H_6 as reductant (SCR inlet temperature = 405 °C); **b** 1 % CO as reductant (SCR inlet temperature = 305 °C). Feed: lean (360 s): 300 ppm NO, 8 % O_2, 5 % CO_2, 5 % H_2O, N_2 as balance; rich (30 s): 300 ppm NO, CO or C_3H_6 as indicated, 5 % CO_2, 5 % H_2O, N_2 as balance; GHSV = 30,000 h^{-1}. The *dotted lines* indicate the time at which the measured concentration of reductant (C_3H_6 or CO) at the LNT outlet exceeds 10 ppm

400 °C. However, the fact that significant N_2O conversion still occurred (>80 %) implies that N_2O decomposition can occur in this temperature range in the absence of reductant.

Numerous studies [36–38] have shown that N_2O breakthrough in LNT catalysts occurs before the breakthrough of the reductant or the NH_3 generated in the LNT. This is consistent with the formation of N_2O in the leading edge of the reduction front in a reaction which occurs in close association with removal of oxygen from the surface of the Pt particles via reaction with the reductant. Under these conditions, the local reductant:NO stoichiometry at Pt is low due to the simultaneous release of NO_x and consumption of reductant in the reaction front by stored oxygen, including that on the oxidized Pt particles. Low reductant:NO ratios are known to favor the formation of N_2O [39]. Figure 5 depicts the concentrations of the main species measured between the LNT and SCR catalysts upon switching from lean to rich conditions, the reductant being C_3H_6. For this experiment slow cycling conditions were used (360 s lean and 30 s rich) in order to enhance the temporal resolution of events. As expected, the concentration profiles in Fig. 5 confirm that N_2O and NO break through the LNT immediately after the lean to rich transition, while a slight delay is evident before the appearance of C_3H_6 and NH_3.

Focusing on N_2O, Fig. 6a compares the measured N_2O concentrations measured behind the LNT and SCR catalysts as a function of time for the slow cycling experiment using C_3H_6 as the reductant, while Fig. 6b shows the results obtained in an analogous experiment using 1 % CO as reductant. Also shown, as indicated by the dotted lines, is the approximate time at which the first trace (>10 ppm) of reductant (C_3H_6 or CO as appropriate) breaks through. From these plots it is evident that a degree of N_2O conversion occurs over the SCR catalyst before the reductant has broken through the LNT catalyst, implying that N_2O decomposition is occurring in the absence of reductant. Note that in these cases the possibility that N_2O reacts with NH_3 stored on the catalyst can be excluded on the basis that significant NO_x slip is observed immediately prior to the lean to rich transition (see Fig. 5), implying that NH_3 present on the SCR catalyst at the beginning of the lean phase has been consumed by this time. Upon breakthrough of the reductant N_2O reduction can commence, which as the data in Fig. 4 imply, occurs at a much lower temperature for H_2 than for CO or C_3H_6. It is also noteworthy that N_2O conversions over the SCR catalyst were found to be lower under the slow cycling

conditions than under fast (60 s lean/5 s rich) cycling. This is explained by the longer times required for reductant breakthrough under slow cycling conditions, this being a consequence of the increased amount of stored NO_x; hence the reductant front propagates more slowly through the LNT and there is comparatively less temporal overlap of the N_2O and reductant in the LNT effluent. Consequently, the measured N_2O conversion corresponding to Fig. 6a was 46 %, whereas the corresponding N_2O conversion measured under fast cycling at similar SCR inlet temperatures was ~88 %.

Finally, the possibility must be considered that N_2O can react with NO over the SCR catalyst, the latter breaking through the LNT catalyst at the same time as the N_2O (Fig. 5). The promotion of N_2O decomposition by NO has previously been reported for Cu–ZSM-5 [22, 23] as well as for Fe–zeolites [25, 27, 28]. The decomposition of N_2O yields N_2 and adsorbed O atoms, high temperatures being required for the associative desorption of these atoms to produce O_2. Indeed, it has been proposed that the recombination of these O atoms controls the overall rate of decomposition. Reductants such as H_2 and CO accelerate this rate by scavenging the adsorbed O, i.e.:

$$N_2O + {}^* \rightarrow N_2 + O^* \quad (1)$$

$$O^* + H_2 \rightarrow H_2O + {}^* \quad (2)$$

Similarly, NO can react with adsorbed O to produce NO_2, which leads to the following stoichiometric process:

$$N_2O + NO \rightarrow N_2 + NO_2 \quad (3)$$

Consequently, it can be expected that N_2O decomposition over the Cu–zeolite catalyst used in our work is similarly promoted by NO. In order to ascertain the effectiveness of the various possible reductants involved in the mitigation of N_2O emissions from the LNT–SCR system, steady-state experiments were performed, the results of which are detailed below.

3.3 Steady-State N_2O Reduction Over SCR Catalyst

Initial steady-state, continuous flow N_2O reduction experiments were conducted in the absence of water using CO, C_3H_6, H_2 and NH_3 reductants. The resulting N_2O conversion data are summarized in Fig. 7a. As shown, in the absence of reductant the N_2O decomposition reaction lights off at relatively high temperature, 50 % N_2O conversion being reached at 400 °C and a maximum conversion of 96 % being attained at 500 °C. In the presence of reductants (1 % H_2, 6,666 ppm NH_3, 1 % CO or 3,333 ppm C_3H_6) N_2O conversion is considerably improved, H_2 being significantly more active in N_2O reduction than CO or C_3H_6. 50 % N_2O conversion was reached at 210 °C using H_2 as the reductant, whereas the corresponding temperatures for NH_3, CO and C_3H_6 were ~290, 375 and 390 °C, respectively.

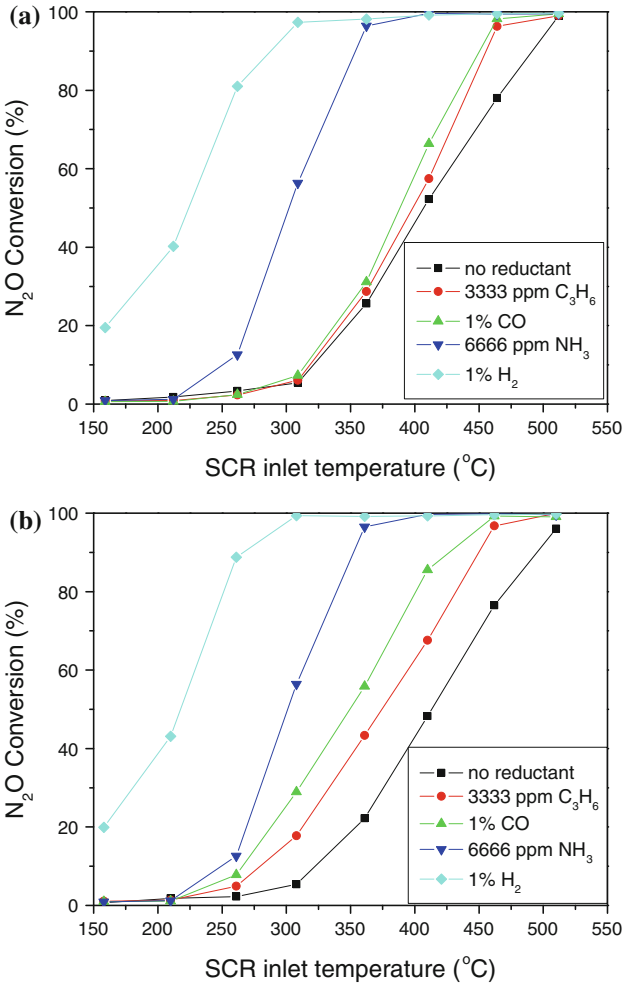

Fig. 7 N_2O reduction with different reductants over SCR catalyst under continuous flow conditions: **a** without H_2O in feed; **b** with 5 % H_2O in feed. Feed: 100 ppm N_2O, 5 % CO_2, 1 % H_2 or 1 % CO or 3,333 ppm C_3H_6 or 6,666 ppm NH_3 as reductant, H_2O as indicated, N_2 as balance; GHSV = 30,000 h^{-1}

Figure 7b shows the corresponding N_2O conversion data obtained with 5 % H_2O added to the feed. Using H_2 and NH_3 as the reductants, N_2O conversion is unaffected by the presence of water, while N_2O decomposition in the absence of reductant is also virtually unaffected. In contrast, water exhibits a promoting effect on N_2O conversion when CO or propene is used as the reductant. This suggests that the reductant in the latter cases is actually H_2; in the case of CO, this is generated in situ via the water–gas shift reaction, while C_3H_6 can be converted to a mixture of CO_2 and H_2 via steam reforming and water–gas shift reactions, i.e.:

$$C_3H_6 + 3H_2O \rightarrow 3CO + 6H_2 \quad (4)$$

$$C_3H_6 + 6H_2O \rightarrow 3CO_2 + 9H_2 \quad (5)$$

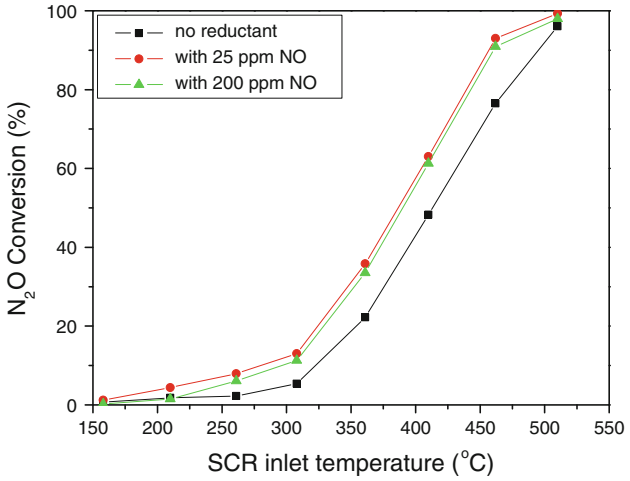

Fig. 8 N_2O decomposition in the presence of NO over SCR catalyst under continuous flow conditions. Feed: 100 ppm N_2O, NO as indicated, 5 % CO_2, 5 % H_2O, N_2 as balance; GHSV = 30,000 h^{-1}

$$CO + H_2O \rightarrow H_2 + CO_2 \quad (6)$$

Comparison of the N_2O conversion profiles with those for CO and C_3H_6 (data not shown) reveals that N_2O reduction exactly tracks the conversion of CO and C_3H_6 for at least the first 40 % of the reductant conversion, even though the reductant is present in huge excess; this is consistent with N_2O reduction lighting off with the water–gas shift reaction in the one case and with the steam reforming reaction in the other. In the case of NH_3, decomposition of NH_3 to N_2 and H_2 represents the only pathway for NH_3 consumption other than oxidation by N_2O. However, NH_3 conversion does not exceed 4 % at any temperature up to 500 °C, which indicates that NH_3 itself functions as the reductant, rather than H_2.

Finally, Fig. 8 shows data comparing N_2O decomposition in the absence of a reductant with decomposition performed in the presence of 25 and 200 ppm of NO. From these results it is evident that NO does indeed exert a modest promoting effect on N_2O decomposition, as described in the literature [22, 23, 25, 27, 28]. The simultaneous formation of NO_2 was observed in these experiments, although the amount measured was consistently below that expected based on the reaction stoichiometry depicted in Eq. 3 (data not shown), even when allowing for possible decomposition of NO_2 to the mixture of NO and NO_2 predicted by thermodynamics. Furthermore, increasing the mole ratio of NO:N_2O in the feed from 0.25 to 2.0 did not increase the N_2O conversion. These results are consistent with previous studies on Fe–ZSM-5 [27, 28] and indicate that NO exerts a catalytic action, rather than simply functioning as a stoichiometric reductant. Indeed, Pérez-Ramírez et al. [28] have suggested that the role of adsorbed NO may be to facilitate migration of adsorbed oxygen through NO_2 intermediates, thereby enhancing the recombination of O_2.

4 Conclusions

The results from this study highlight a significant benefit of coupled LNT–SCR systems, namely, the mitigation of N_2O emissions generated over the LNT during rich purging by the downstream Cu–chabazite SCR catalyst. Experiments performed under lean–rich cycling conditions using H_2, CO and C_3H_6 for the reduction of stored NO_x showed that the selectivity of the LNT catalyst to N_2O is greater when using CO as the reductant, as compared to H_2 or C_3H_6. Immediately after the switch to rich conditions, N_2O decomposition occurs on the SCR catalyst in the absence of reductant. Steady-state data indicate that this process is weakly promoted by NO which breaks through the LNT at the same time as the N_2O. Upon subsequent breakthrough of the reductant, and any NH_3 generated over the LNT, N_2O reduction can occur. Steady-state experiments reveal H_2 to be an excellent reductant, the order $H_2 > NH_3 > CO > C_3H_6$ being observed for efficacy of N_2O reduction.

Acknowledgments This project was funded by the U.S. Department of Energy (DOE) under award No. DE-EE0000205. The authors thank BASF for providing the catalysts used in this study. Dr. R. McCabe of Ford Motor Co. is thanked for helpful discussions.

References

1. Epling WS, Campbell LE, Yezerets A, Currier NW, Parks JE II (2004) Catal Rev 46:163
2. Gabrielsson PLT (2004) Top Catal 28(1–4):177
3. Dykes EC (2008) SAE Technical Paper 2008-01-2642
4. Corbos EC, Haneda M, Courtois X, Marecot P, Duprez D, Hamada H (2009) Appl Catal A 365:187
5. Xu L, McCabe R, Ruona W, Cavataio G (2009) SAE Technical Paper 2009-01-0285
6. Weibel M, Waldbüsser N, Wunsch R, Chatterjee D, Bandl-Konrad B, Krutzsch B (2009) Top Catal 52:1702

7. Zukerman R, Vradman L, Herskowitz M, Liverts E, Liverts M, Massner A, Weibel M, Brilhac JF, Blakeman PG, Peace LJ (2009) Chem Eng J 155:419
8. Xu L, McCabe R, Dearth M, Ruona W (2010) SAE Technical Paper 2010-01-0305
9. Chatterjee D, Koči P, Schmeisser V, Marek M, Weibel M, Krutzsch B (2010) Catal Today 151:395
10. Bonzi R, Lietti L, Castoldi L, Forzatti P (2010) Catal Today 151:376
11. Lindholm A, Sjövall H, Olsson L (2010) Appl Catal B 98:112
12. Wang J, Ji Y, He Z, Crocker M, Dearth M, McCabe RW (2012) Appl Catal B 111–112:562
13. Ravishankara AR, Daniel JS, Portmann RW (2009) Science 326:123
14. Kapteijn F, Rodriguez-Mirasol J, Moulijn JA (1996) Appl Catal B 9:25
15. Pérez-Ramírez J (2007) Appl Catal B 70:31
16. Abdulhamid H, Fridell E, Skoglundh M (2004) Top Catal 30/31:161
17. Epling WS, Yezerets A, Currier NW (2007) Appl Catal B 74:117
18. Clayton RD, Harold MP, Balakotaiah V (2008) Appl Catal B 81:161
19. Choi JS, Partridge WP, Pihl JA, Daw CS (2008) Catal Today 136:173
20. Ji Y, Easterling V, Graham U, Fisk C, Crocker M, Choi JS (2011) Appl Catal B 103:413
21. Elizundia U, Duraiswami D, Pereda-Ayo B, López-Fonseca R, González-Velasco JR (2011) Catal Today 176:324
22. Pirone R, Ciambelli P, Palella B, Russo G (2000) Stud Surf Sci Catal 130:911
23. Turek T (1998) J Catal 174:98
24. Dandekar A, Vannice MA (1999) Appl Catal B 22:179
25. Kapteijn F, Marban G, Rodriguez-Mirsol J, Moulijn JA (1997) J Catal 167:256
26. Yamada K, Pophal C, Segawa K (1998) Microporous Mesoporous Mater 21:549
27. Kaucký D, Sobalik Z, Schwarze M, Vondrová A, Wichterlová B (2006) J Catal 238:293
28. Pérez-Ramírez J, Kapteijn F, Mul G, Moulijn JA (2002) J Catal 208:211
29. Devadas M, Kröcher O, Elsener M, Wokaun A, Söger N, Pfeifer M, Demel Y, Mussmann L (2006) Appl Catal B 67:187
30. van den Brink RW, Booneveld S, Pels JR, Bakker DF, Verhaak MJFM (2001) Appl Catal B 32:73
31. Pophal C, Yogo T, Tanabe K, Segawa K (1997) Catal Lett 44:271
32. Yamada K, Kondo S, Segawa K (2000) Microporous Mesoporous Mater 35–36:227
33. Kameoka S, Yuzaki K, Takeda T, Tanaka S, Ito S, Miyadera T, Kunimori K (2001) Phys Chem Chem Phys 3:256
34. Chaki T, Arai M, Ebina T, Shimokawabe M (2005) J Mol Catal A 227:187
35. Shi C, Ji Y, Graham UM, Jacobs G, Crocker M, Zhang Z, Wang Y, Toops TJ (2012) Appl Catal B 119–120:183
36. Castoldi L, Nova I, Lietti L, Forzatti P (2004) Catal Today 96:43
37. Tonkyn RG, Disselkamp RS, Peden CHF (2006) Catal Today 114:94
38. Cumaranatunge L, Mulla SS, Yezerets A, Currier NW, Delgass WN, Ribeiro FH (2007) J Catal 246:29
39. Pihl JA, Parks II JE, Daw CS, Root TW (2006) SAE Technical Paper 2006-01-3441